

Copy
NASA TM X-86

NASA TM X-86



*W 07
310 540
p 34*

TECHNICAL MEMORANDUM

X-86

EXPERIMENTAL INVESTIGATION OF A 0.35 HUB-TIP RADIUS
RATIO TRANSONIC AXIAL FLOW ROTOR DESIGNED FOR
40 POUNDS PER SECOND PER SQUARE FOOT WITH
A DESIGN TIP DIFFUSION FACTOR OF 0.20

By Paul T. Yasaki and John C. Montgomery

Lewis Research Center
Cleveland, Ohio

CLASSIFICATION CHANGED TO
UNCLASSIFIED - AUTHORITY:
NASA - EFFECTIVE DATE
SEPTEMBER 14, 1992

CLASSIFIED DOCUMENT - TITLE UNCLASSIFIED

This material contains information affecting the national defense of the United States within the meaning of the espionage laws, Title 18, U.S.C., Secs. 793 and 794, the transmission or revelation of which in any manner to an unauthorized person is prohibited by law.

NATIONAL AERONAUTICS AND SPACE ADMINISTRATION
WASHINGTON

September 1959

TECHNICAL MEMORANDUM X-86

EXPERIMENTAL INVESTIGATION OF A 0.35 HUB-TIP RADIUS
RATIO TRANSONIC AXIAL FLOW ROTOR DESIGNED FOR
40 POUNDS PER SECOND PER SQUARE FOOT WITH
A DESIGN TIP DIFFUSION FACTOR OF 0.20*

By Paul T. Yasaki and John C. Montgomery

SUMMARY

In order to determine the effect of a low design diffusion factor on the performance of a transonic axial-flow compressor rotor, a high-specific-flow rotor with a 0.35 hub-tip radius ratio was designed, fabricated, and tested. This rotor used a design tip diffusion factor of 0.20 with a design corrected specific weight flow of 40 pounds per second per square foot of frontal area, a total-pressure ratio of 1.27, and an adiabatic efficiency of 0.96. The design, rotor performance, and blade element performance are presented with a discussion on rotor shock losses and a comparison with a similarly designed rotor with a tip diffusion factor of 0.35.

At the design corrected tip speed of 1100 feet per second, a peak rotor adiabatic efficiency of 0.88 was attained at a corrected specific weight flow of 39 pounds per second per square foot of frontal area with a mass-averaged total-pressure ratio of 1.27. The blade element tip diffusion factor was 0.28, which is 0.08 higher than the design value of 0.20. Peak efficiencies of 0.95, 0.91, 0.89, and 0.85 were obtained at 70, 80, 90, and 110 percent of design speed, respectively.

Comparison of the performance of the rotor reported herein and a similarly designed rotor with increased blade loading indicates that higher blade loading results in a more desirable rotor because of a higher pressure ratio and equivalent efficiency. Computed values of shock losses at the rotor tip section indicate that the losses at peak efficiency are primarily a function of shock losses since the profile losses are only a small percentage of the total loss.

*Title, Unclassified.



At design speed and weight flow, stator losses obtained from typical stator loss curves indicated that a stage total-pressure ratio of 1.26 and an efficiency of 0.85 can be expected. This computed drop in total-pressure ratio and efficiency amounts to approximately 1.0 and 3.0 percent, respectively.

INTRODUCTION

The investigation of transonic rotors, such as reported in references 1 to 5, indicated that the efficiency of the rotor tip section decreases markedly with increased speed. The decrease in efficiency at the tip section has been attributed to a combination of losses due to blade loading and shock wave formations. Reference 4 shows that tip section losses could be reduced by reducing the blade loading. In reference 4 the reduced tip section blade loading was accomplished by tapering the outer passage inward across the rotor. In so doing, the performance of two blade tip sections with identical inlet Mach numbers was obtained. However, the blade-surface relative Mach numbers varied with the change in the blade tip section camber angle, and with the three-dimensional flow introduced by the tapered wall contour.

In order to investigate further the effects of blade loading on the performance of tip sections of transonic rotors, two rotors with the same inlet conditions and employing similar design technique and limitations with the exception of blade loading were designed and tested. Double-circular-arc blade sections were used for both designs so that blade surface Mach numbers varied systematically with blade loading. Both rotors were designed for a 0.35 hub-tip radius ratio and an equivalent weight flow of 40 pounds per second per square foot of frontal area. Both rotors utilized a tapered tip section and constant radial energy addition. As a measure of blade loading, the design technique makes use of the diffusion factor, as developed in reference 6. One rotor (ref. 5) was designed for a 0.35 diffusion factor at the tip and the other rotor was designed for a 0.20 diffusion factor at the tip.

Complete performance tests were made on both rotors in order to provide additional information on transonic rotors and to permit a study of the effect of blade loading and surface Mach number on the losses of the rotor tip sections. The design and performance of the rotor with the 0.35 tip element diffusion factor is presented in reference 5. The design and performance of the rotor with a 0.20 diffusion factor and a comparison with the rotor with a 0.35 diffusion factor are presented herein.

ROTOR DESIGN

Velocity Diagram Calculations

In the design of the compressor inlet stage reported herein, the following conditions were selected:

- (1) A hub-tip radius ratio of 0.35 at the rotor inlet with an inlet tip diameter of 14 inches
- (2) A specific weight flow of 40 pounds per second per square foot of frontal area with boundary-layer blockage factors at the rotor inlet and outlet of 0.98 and 0.97, respectively
- (3) Rotor inlet tip speed of 1100 feet per second
- (4) Rotor chord of 2 inches with a tip solidity of approximately 1.0
- (5) Tip taper across the rotor (expressed as a ratio of outlet tip radius to inlet tip radius)
- (6) Rotor tip diffusion factor of approximately 0.20
- (7) An average axial velocity ratio of approximately 1.0 across the rotor
- (8) Radially constant energy addition
- (9) No inlet whirl (no guide vanes)
- (10) Radially constant value of blade-element relative total-pressure-loss coefficient

The design parameters of this rotor were the same as those used in reference 5, except for the tip diffusion factor and the amount of tip taper across the rotor. The diffusion factor was decreased from 0.35 to 0.20 and the tip taper ($r_{t,2}/r_{t,1}$) was changed from 0.97 to 0.98. (All symbols are defined in appendix A.) The tip taper was changed to 0.98 because of the lower density increase across the low loading blade row. Inasmuch as the design weight flow, wheel speed, and blockage factors are the same, the design inlet flow parameters except incidence angle of the two rotors are the same; however, the difference in diffusion factor changed the outlet flow parameters.

The calculation procedure to determine the radial distribution of rotor outlet axial velocity was the same as that used and discussed in references 5 and 7. The preceding computations using an assumed efficiency

of 0.96 resulted in a design rotor over-all pressure ratio of 1.27 as compared with 1.51 for the rotor of reference 5. The radial variations of specific flow parameters are included in table I.

Blade Selection

Double-circular-arc blades with leading and trailing edge radii of 0.010 inch were employed. From strength considerations, the maximum thickness ratio of the rotor was selected to vary from 8 percent of the chord at the hub to 5 percent at the tip.

With the design velocity diagrams determined, the blade sections that would produce the desired velocity diagrams were selected. The design rules of reference 8 were used to determine the incidence angle, deviation angle, and camber angle for each blade section.

The resultant values of the rotor blade design configuration and geometry are presented in table I for the blade sections located along conical surfaces at 10, 30, 50, 70, and 90 percent of the passage height from the outer wall.

Rotor Outlet Annulus

For the test of the rotor alone, the annulus at the rotor outlet (fig. 1(a)) was enlarged at the outer wall to prevent choking downstream of the rotor. The annulus was gradually enlarged after the rotor outlet measuring station to allow the design value of wall curvature to exist through the rotor as far as permissible. In this manner the effect of enlarging the outlet passage minimized the possibility of affecting the design axial velocity distribution after the rotor.

APPARATUS AND PROCEDURE

The rotor testing facility is shown as a schematic diagram in figure 1(b), with stations 0, 1, and 2 indicating the axial measuring stations. The compressor installation and instrumentation are the same as in reference 5, and a detailed discussion can be obtained from this reference.

The testing procedure included over-all and blade element performance data points at 70, 80, 90, 100, and 110 percent of design speed. Inlet pressure was maintained at 20 inches of mercury absolute for all speeds. Weight flow was varied from the maximum obtainable down to a value where blade vibrations were encountered, or to a point where the blade tip section adiabatic efficiency decreased to approximately 70 percent.

In the computation of blade element performance parameters, the streamlines were assumed to lie along conical sections connecting points of equal percentage of the passage height at rotor inlet and outlet. The major radial positions presented and discussed are at 10, 30, 50, 70, and 90 percent of the passage height and are noted in table I as radial positions A, B, C, D, and E, respectively. The specific discussion within this report designates the 10 percent point (radial position A) as the tip section and the 90 percent point (radial position E) as the hub section; however, the other radial positions are indicated by their respective letters. The symbols and equations used in computing the rotor performance are included in appendixes A and B.

RESULTS AND DISCUSSION

Rotor Over-All Performance

The rotor over-all performance is presented in figure 2 in which mass-averaged total-pressure ratio and adiabatic efficiency are plotted as a function of the rotor-inlet corrected specific weight flow. The design total-pressure ratio of 1.27 was obtained at a weight flow of 39.0 pounds per second per square foot of frontal area and at an adiabatic efficiency of 0.88. At the design pressure ratio, the specific weight flow of 39.0 pounds per second was 2.5 percent less than the design value of 40 pounds per second. Peak efficiency at design speed occurred at the design pressure ratio and was also 0.88. The maximum pressure ratio attained at design speed was 1.33, while the maximum weight flow was 39.2 pounds per second per square foot of frontal area.

The peak values of efficiency, pressure ratio, and weight flow obtained at 110 percent of design speed were 0.85, 1.43, and 40.2, respectively. The peak efficiencies obtained at 70, 80, and 90 percent of design speed were 0.95, 0.91, and 0.89, respectively.

Flow Parameters

The flow parameters (rotor inlet, rotor outlet, and blade element), which are used to compare the design and actual flow conditions, are presented in figures 3 to 5.

The rotor-inlet and -outlet flow parameters are plotted against their respective radii in figures 3 to 4(c) for 100, 110, and 90 percent of design speed. The various flow parameters are presented for three values of weight flow at each speed: the near-maximum weight flow, the near-peak efficiency weight flow, and the lowest weight flow. At design speed (figs. 3(a) and 4(a)) the design values of the respective flow parameters are included for comparison purposes. The blade element flow

parameters are plotted against incidence angle in figure 5 and are presented for 70, 80, 90, 100 and 110 percent of design speed. The extensive flow parameter data are presented to provide additional information on the performance of transonic rotors. The flow parameter curves in general are self-explanatory and therefore the discussion of them will be kept to a minimum.

Inlet flow parameters. - The rotor inlet flow parameters of inlet axial Mach number, inlet relative Mach number, and inlet relative air angle are presented in figure 3. At design speed (fig. 3(a)) the radial distribution of inlet axial Mach number is similar to the design distribution but its magnitude is low because the design weight flow of 40 pounds per second per square foot of frontal area was not attained. It therefore appears that the method employed for calculating the rotor-inlet axial velocity distribution is quite satisfactory.

Outlet flow parameters. - The rotor-outlet flow parameters of dimensionless work coefficient, adiabatic efficiency, total-pressure ratio, relative total-pressure loss coefficient, deviation angle, relative outlet Mach number, absolute outlet Mach number, axial velocity ratio, and diffusion factor are plotted against rotor outlet radius in figure 4. At design speed (fig. 4(a)) the design values of the respective flow parameters are included.

In the design procedure the energy addition (work coefficient) and the total-pressure loss coefficient were assumed constant over the radial passage height. As shown in figure 4(a), however, both the energy addition and the total-pressure loss coefficient increased from the rotor hub to the rotor tip at the near-peak-efficiency weight flow. Only at the maximum weight flow were the design values and distribution of energy addition and total-pressure loss coefficient nearly obtained. The energy addition and the total-pressure loss coefficient combine to give the resultant total-pressure ratio and efficiency, as shown in figure 4(a).

Obtaining the design energy addition is primarily a function of obtaining the design values of the axial-velocity and blade deviation angles. The design values of deviation angle (fig. 4(a)) were obtained from the design rules of reference 8. The design axial-velocity ratio (fig. 4(a)) was obtained by the method outlined in references 5 and 7 in which constant radial values of the total-pressure loss coefficient and energy addition were assumed.

The deviation angle (fig. 4(a)) was within 2° of the design value from the mean passage to the rotor tip section. At the hub section, however, the deviation angle increased to approximately 6° above the design value. The increase at the hub may be attributed to the low hub-tip ratio since the design rules were based primarily on rotors having hub-tip ratios of 0.4 and higher. Of the 17 rotors used in reference 8 to formulate the design rule, only one rotor had a hub-tip ratio as low as 0.4.

The axial-velocity ratio (fig. 4(a)) varied from the design condition primarily because the conditions of constant angular momentum (or constant energy addition since inlet whirl was zero) and constant total-pressure loss coefficient were not as was assumed. Although the design method employed for calculating the inlet and the outlet axial-velocity distribution were the same, the method was only satisfactory at the inlet where the assumed design conditions of constant angular momentum and constant total-pressure loss coefficient were obtained.

The rotor flow parameters for 90 and 110 percent of design speeds are presented in figures 4(b) and (c). The radial distribution of these flow parameters in general did not differ from the design speed radial distribution, but varied in level as would be expected for the change in rotor speed.

Blade element performance. - The blade element performance parameters (deviation angle, relative total-pressure loss coefficient, relative inlet Mach number, diffusion factor, axial velocity ratio, efficiency, and dimensionless work coefficient) are presented in figure 5 as a function of the incidence angle. The data are presented at the five radial positions (A, B, C, D, E, see table I) for 70, 80, 90, 100, and 110 percent of design speed. The extensive blade element data are presented to further supplement the published data on transonic rotor blade performance.

COMPARISON OF LOSS COEFFICIENTS

The variation of rotor tip relative total-pressure loss coefficient and the calculated shock loss coefficient with inlet relative Mach number for the near-peak-efficiency weight flow points at 90, 100, and 110 percent of design speed are presented in figure 6. Similar data points for the rotor of reference 5 are also plotted to form a comparison of losses between the two rotors. The computed shock loss coefficient was obtained using the method outlined in reference 9.

The loss coefficients for this rotor (fig. 6) were noticeably lower than those for the rotor with a diffusion factor of 0.35. With the same inlet relative Mach number for the two rotors, the lower camber angle of the lower loaded rotor limits the expansion and acceleration of the flow, thereby decreasing the blade suction surface Mach number and decreasing the shock loss.

As shown in figure 6, the shock loss (as computed) is the major portion of the total loss. In general, the profile loss remained relatively constant and the shock loss increased sharply as Mach number was increased. For a given inlet relative Mach number at peak efficiency flow (fig. 6), it appears that the loss coefficient is primarily a function of shock losses, because the profile losses are only a small percentage of the total losses.



COMPARISON OF ROTOR PERFORMANCE

A comparison of rotor performance is presented in figure 7 in which adiabatic efficiency, total-pressure ratio, and flow range are plotted against the percentage of design speed. The efficiency and pressure ratio points were selected at the near-maximum-efficiency weight flow points at their respective speeds. The flow range is presented as percentage of maximum weight flow; however, it should be recalled the minimum weight flow defined herein is the point where blade vibrations were encountered or tip element efficiency dropped to 0.70, whichever occurred first.

As shown in figure 11, the peak efficiency of the rotor with a 0.35 diffusion factor was greater than the peak efficiency of the rotor with a 0.20 diffusion factor at all speeds except for the condition of 110 percent of design speed. Although the loss factor of the rotor with a 0.35 diffusion factor increased with diffusion factor for a given inlet relative Mach number (fig. 6), the energy addition also increased. Since efficiency is a function of the total-pressure loss coefficient and the energy addition, the net result was an increase in efficiency. Obviously, the pressure ratio for the rotor with a 0.35 diffusion factor was higher because of the combination of higher loading and better efficiency.

From the viewpoint of off-design operation of multistage units and also of inlet flow distortions, the range parameter is of interest. As mentioned previously, sufficient data were not obtained to provide true and accurate values of flow range parameter from which a conclusive comparison could be made. However, the range parameter presented in figure 7 indicates that the lightly loaded rotor at high speeds has a greater range of flow; but at the slow speeds this advantage is almost negligible.

Although stators were not used in conjunction with the rotor with a 0.2 diffusion factor, their performance was estimated so that a comparison of the over-all stage performances of the two inlet stages could be made. In reference 10, it is shown that at design speed the stator blades for the rotor with a 0.35 diffusion factor decreased the rotor efficiency 5 percent and the total-pressure ratio 3 percent. Primarily because of the reduced Mach numbers at the rotor outlet, it was estimated that under ideal conditions the stator blades for the rotor with a 0.20 diffusion factor at design speed would reduce the rotor efficiency 3 percent and the total-pressure ratio 1 percent. In comparing the over-all stage performance of the rotor with a 0.35 diffusion factor with the estimated over-all stage performance of the rotor with a 0.2 diffusion factor for peak efficiency at design speed, the efficiencies were equal at 0.85, whereas the total-pressure ratio of the highly loaded rotor was 1.45 compared with 1.26 for the lower loaded rotor.



In view of the previous comparisons it appears that the more highly loaded rotor of reference 5 is more desirable because of a higher total-pressure ratio, with the efficiency and the weight flow range of the two rotors equivalent. Also, of great concern from the standpoint of weight and production is that the more highly loaded rotor could possibly mean the elimination of a stage from a compressor.

SUMMARY OF RESULTS

The results obtained from the experimental investigation of the 0.35 hub-tip radius ratio rotor with a design tip diffusion factor of 0.20 are as follows:

1. At the design corrected tip speed of 1100 feet per second, the design total-pressure ratio of 1.27 was attained at a corrected specific weight flow of 39.0 pounds per second per square foot of frontal area with an adiabatic temperature-rise efficiency of 0.88. The maximum weight flow and pressure ratio attained at design speed were 39.2 pounds per second per square foot of frontal area and 1.33, respectively.

2. The peak values of efficiency, pressure ratio, and weight flow attained at 110 percent of design speed were 0.85, 1.43, and 40.2, respectively. The peak efficiencies attained at 70, 80, and 90 percent of design speed were 0.95, 0.91, and 0.89, respectively.

3. The blade element performance parameters indicated that:

(a) The method employed for determining the axial velocity distributions, which assumes constant energy addition and constant entropy across the passage, was satisfactory at the rotor inlet but was not satisfactory at the rotor outlet where the assumed design conditions were not obtained.

(b) The deviation angle at the rotor hub was as much as 6° greater than the value predicted by the design rules and at all other radial blade positions the agreement was within 2° .

(c) The assumed radially constant relative total-pressure loss coefficient and energy addition were obtained only at the maximum weight flow condition.

4. At peak efficiency flow a comparison of the loss coefficients at the tip section indicates that the loss coefficient is primarily a function of the shock losses since the profile losses are only a small percentage of the total losses.

δ°	deviation angle, angle between outlet-air direction and tangent to mean camber line at trailing edge, deg
η	adiabatic efficiency
θ	ratio of total temperature to NACA standard sea-level temperature of 518.7° R
ρ	flow density, lb/cu ft
σ	solidity
ϕ	blade camber angle, deg
$\bar{\omega}$	relative total pressure loss coefficient

Subscripts:

h	hub
i	ideal
R	rotor
S	shock
sl	sea level
t	tip
v	constant volume
z	axial direction
1	rotor inlet
2	rotor outlet

Superscript:

'	relative
---	----------

APPENDIX B

EQUATIONS FOR THE BLADE ELEMENT AND OVER-ALL PERFORMANCE

Over-All Performance

Mass-averaged temperature-rise adiabatic efficiency:

$$\eta = \frac{T_1 \int_{r_{h,2}}^{r_{t,2}} \rho_2 V_{z,2} r_2 \left[\left(\frac{P_2}{P_1} \right)^{\frac{\gamma-1}{\gamma}} - 1 \right] dr_2}{\int_{r_{h,2}}^{r_{t,2}} \rho_2 V_{z,2} r_2 (T_2 - T_1) dr_2} \quad (1)$$

Mass-averaged total-pressure ratio:

$$\frac{P_2}{P_1} = \left\{ \frac{\int_{r_{h,2}}^{r_{t,2}} \rho_2 V_{z,2} r_2 \left[\left(\frac{P_2}{P_1} \right)^{\frac{\gamma-1}{\gamma}} - 1 \right] dr_2}{\int_{r_{h,2}}^{r_{t,2}} \rho_2 V_{z,2} r_2 dr_2} + 1.0 \right\}^{\frac{\gamma}{\gamma-1}} \quad (2)$$

Rotor Blade Element

Blade element temperature-rise adiabatic efficiency:

$$\eta = \frac{\left(\frac{P_2}{P_1} \right)^{\frac{\gamma-1}{\gamma}} - 1}{\frac{T_2}{T_1} - 1} \quad (3)$$

Relative total-pressure loss coefficient:

$$\bar{\omega} = \left(\frac{P_2}{P_1} \right)_i \left[\frac{1 - \left(\frac{P_2}{P_1} \right) \left(\frac{T_1}{T_2} \right)^{\frac{\gamma}{\gamma-1}}}{1 - \left(1 + \frac{\gamma-1}{2} M_R^2 \right)^{-\frac{\gamma}{\gamma-1}}} \right] \quad (4)$$

where

$$\left(\frac{P_2}{P_1} \right)_i = \left\{ 1 + \frac{\gamma-1}{2} M_R^2 \left[1 - \left(\frac{r_1}{r_2} \right)^2 \right] \right\}^{\frac{\gamma}{\gamma-1}} = 1$$

for a given rotor design and M_R^1 is the wheel rotational Mach number (outlet wheel tangential velocity divided by inlet relative stagnation velocity of sound).

Dimensionless work coefficient:

$$\frac{\Delta H}{U_t^2} = \frac{J g_c p T_{s1} \left(\frac{T_2}{T_1} \right) - 1}{\left(\frac{U_t}{\sqrt{\theta}} \right)^2} \quad (5)$$

Diffusion factor:

$$D = \left(1 - \frac{V_2'}{V_1'} \right) + \frac{V_{\theta,1}' - V_{\theta,2}'}{2\sigma V_1'} \quad (6)$$

REFERENCES

1. Schwenk, Francis C., Lieblein, Seymour, and Lewis, George W., Jr.: Experimental Investigation of an Axial-Flow Compressor Inlet Stage Operating at Transonic Relative Inlet Mach Numbers. III - Blade-Row Performance of Stage with Transonic Rotor and Subsonic Stator at Corrected Tip Speeds of 800 and 1000 Feet per Second. NACA RM E53G17, 1953.
2. Lewis, George W., Jr., Schwenk, Francis C., and Serovy, George K.: Experimental Investigation of a Transonic Axial-Flow-Compressor Rotor with Double-Circular-Arc Air Foil Blade Sections. I - Design, Over-All Performance, and Stall Characteristics. NACA RM E53L21a, 1954.
3. Montgomery, John C., and Glaser, Frederick W.: Experimental Investigation of a 0.4 Hub-Tip Diameter Ratio Axial-Flow Compressor Inlet Stage at Transonic Inlet Relative Mach Numbers. II - Stage and Blade-Element Performance. NACA RM E54I29, 1955.
4. Montgomery, John C., and Glaser, Frederick: Experimental Investigation of a 0.4 Hub-Tip Diameter Ratio Axial-Flow Compressor Inlet Stage at Transonic Inlet Relative Mach Numbers. III - Effect of Tip Taper on Over-All and Blade-Element Performance. NACA RM E55L09, 1956.
5. Montgomery, John C., and Yasaki, Paul T.: Design and Experimental Performance of a 0.35 Hub-Tip Radius Ratio Transonic Axial-Flow-Compressor Rotor Designed for 40 Pounds per Second per Unit Frontal Area. NACA RM E58D17, 1958.
6. Lieblein, Seymour, Schwenk, Francis C., and Broderick, Robert L.: Diffusion Factor for Estimating Losses and Limiting Blade Loadings in Axial-Flow-Compressor Blade Elements. NACA RM E53D01, 1953.
7. Hatch James E., Giamati, Charles C., and Jackson, Robert J.: Application of Radial-Equilibrium Condition to Axial-Flow Turbomachine Design Including Consideration of Change of Entropy with Radius Downstream of Blade Row. NACA RM E54A20, 1954.
8. Robbins, William H., Jackson, Robert J., and Lieblein, Seymour: Blade-Element Flow in Annular Cascades. Ch. VII of Aerodynamic Design of Axial-Flow Compressors, vol. II. NACA RM E56B03a, 1956.



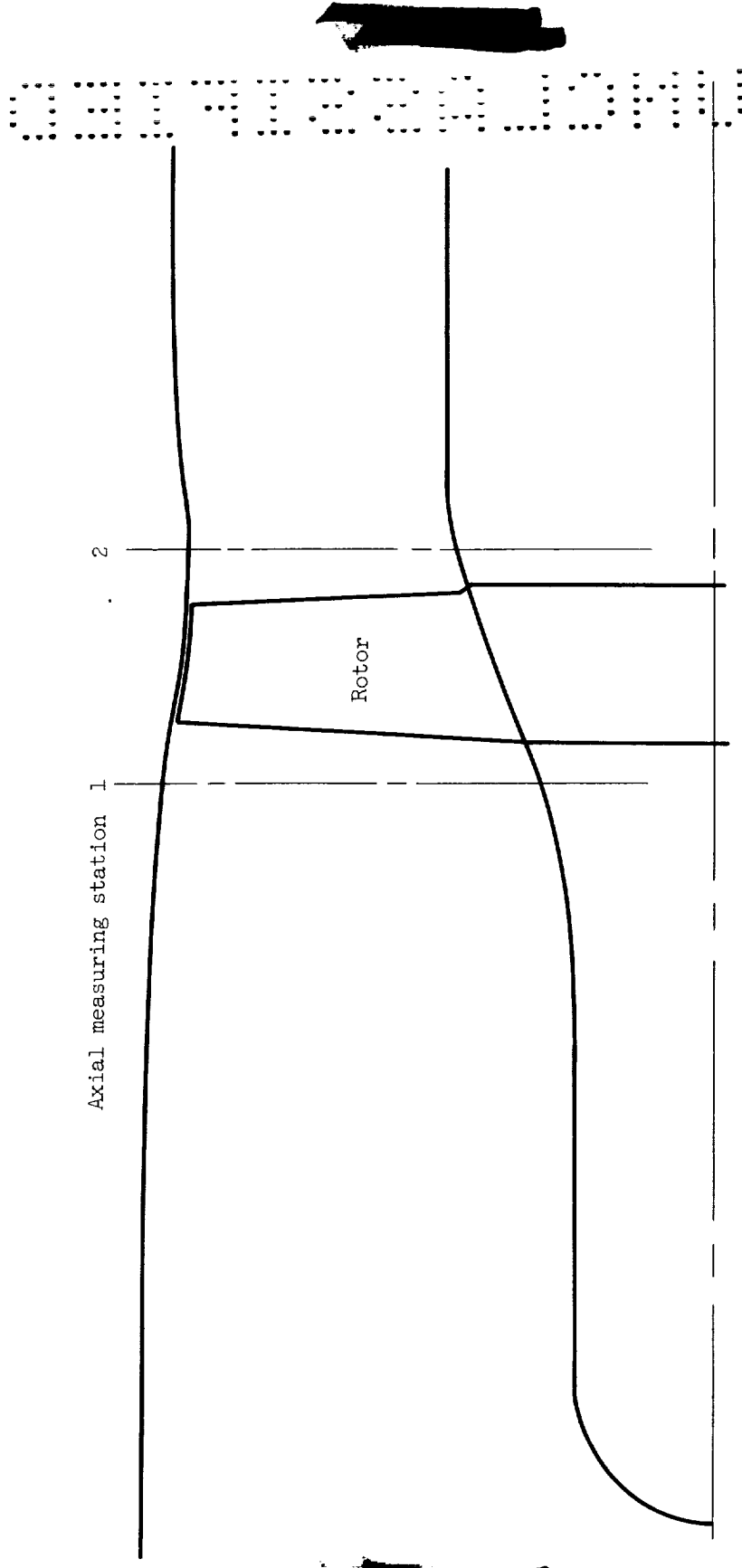
- 
9. Schwenk, Francis C., Lewis, George W., and Hartmann, Melvin J.: A Preliminary Analysis of the Magnitude of Shock Losses in Transonic Compressors. NACA RM E57A30, 1957.
10. Cullom, Richard R., Montgomery, John C., and Yasaki, Paul T.: Experimental Performance of a 0.35 Hub-Tip Radius Ratio Transonic Axial-Flow Compressor Stage Designed for 40 Pounds per Second per Unit Frontal Area. NACA RM E58D04a, 1958.
- 

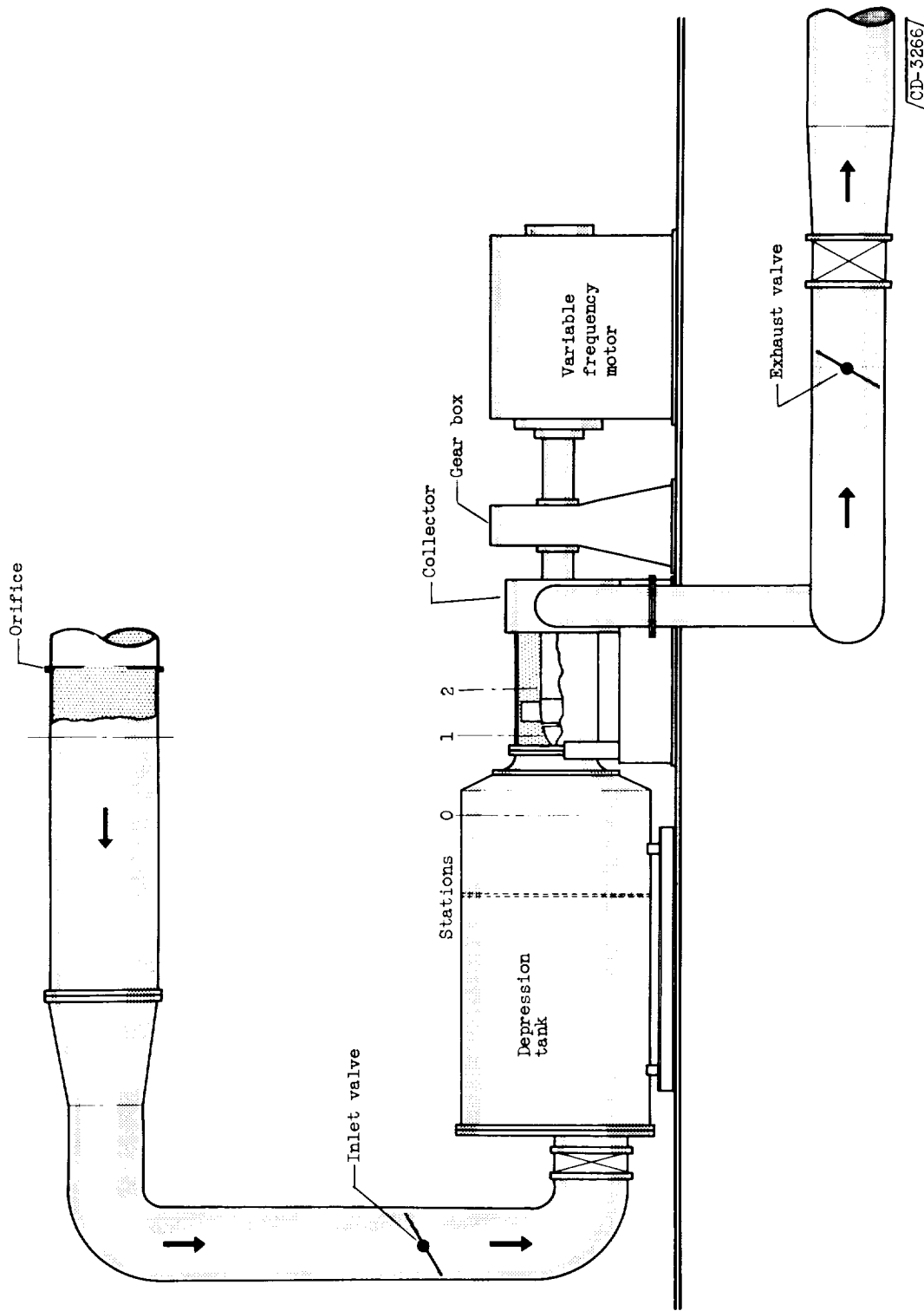
TABLE I. - ROTOR BLADE DESIGN VALUES AND GEOMETRY

Radial position	Passage height from outer wall, percent	Inlet radius, r_1 , in.	Outlet radius, r_2 , in.	Relative inlet air angle, β_1 , deg	Relative outlet air angle, β_2 , deg	Blade thickness ratio, t/c	Solidity, σ	Diffusion factor, D	Blade camber angle, ϕ , deg	Relative inlet Mach number, M_1	Absolute outlet Mach number, M_2	Incidence angle, i , deg	Deflection angle, δ , deg
A	10	6.59	6.50	52.3	42.1	0.053	0.976	0.208	3.1	1.228	0.800	5.7	0.1
B	30	5.67	5.77	46.9	38.3	.059	1.117	.231	.8	1.151	.784	7.3	0.1
C	50	4.75	5.04	41.8	31.5	.065	1.304	.241	2.0	1.059	.784	9.1	0.5
D	70	3.83	4.31	37.0	21.3	.071	1.567	.221	7.3	.942	.600	9.7	2.3
E	90	2.91	3.58	31.9	9.9	.077	1.962	.143	16.2	.809	.641	9.9	4.1



(a) Rotor-outlet annulus.

Figure 1. - Schematic diagram of compressor installation.



(b) Rotor testing facility.
 Figure 1. - Concluded. Schematic diagram of compressor installation.

~~CONFIDENTIAL~~

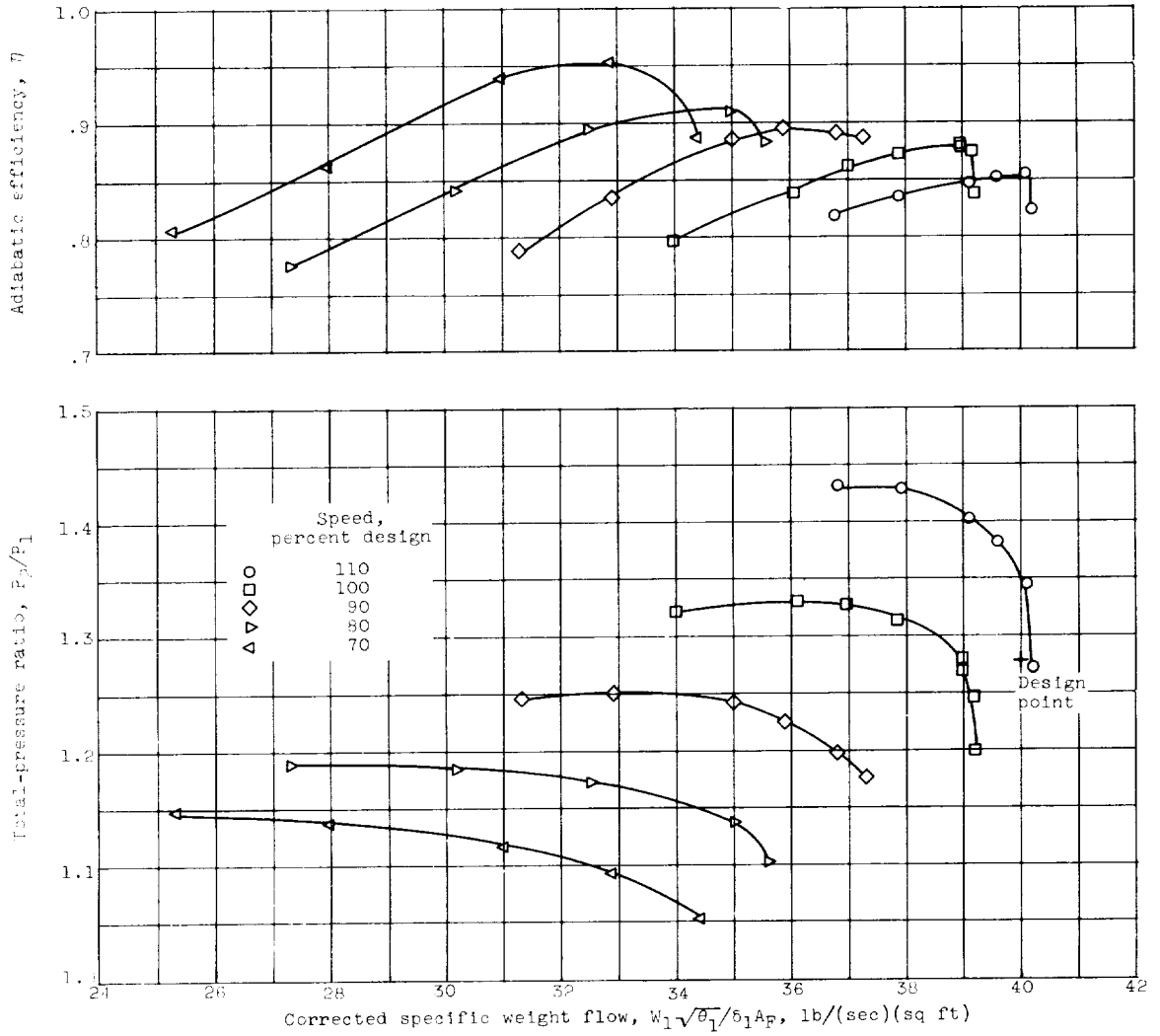
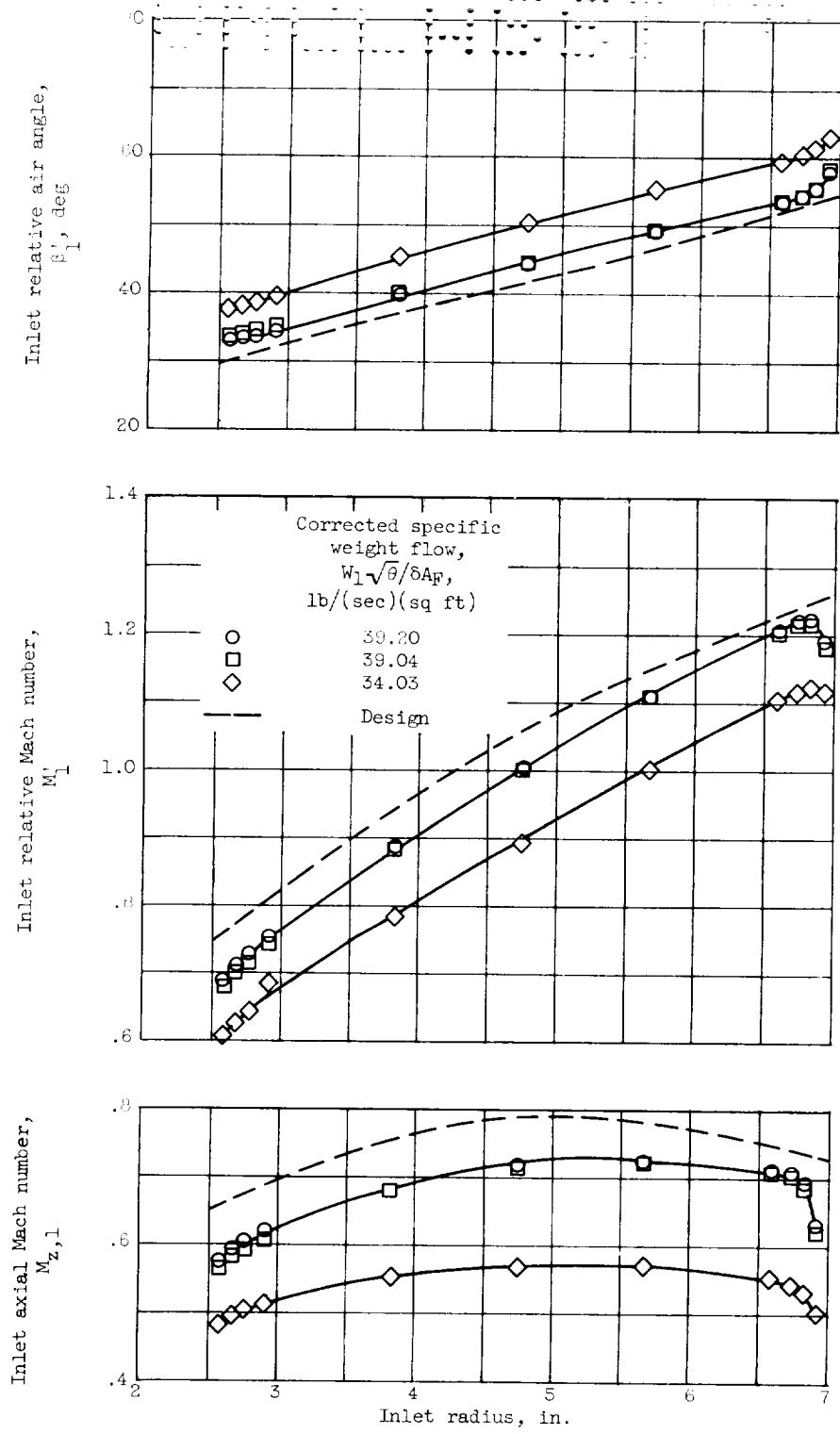


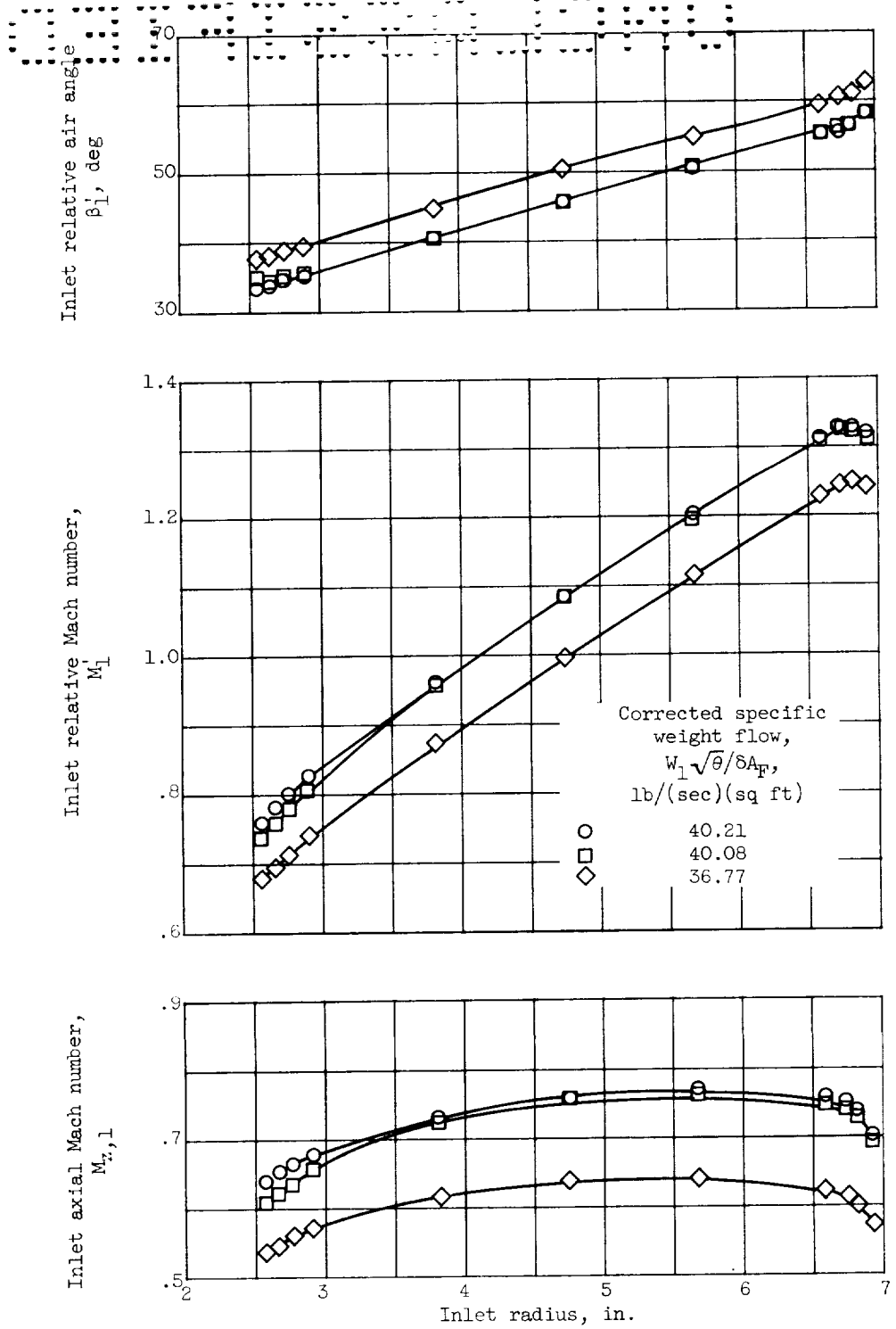
Figure 2 - Mass-averaged over-all performance of rotor with a 0.35 hub-tip radius ratio

~~CONFIDENTIAL~~



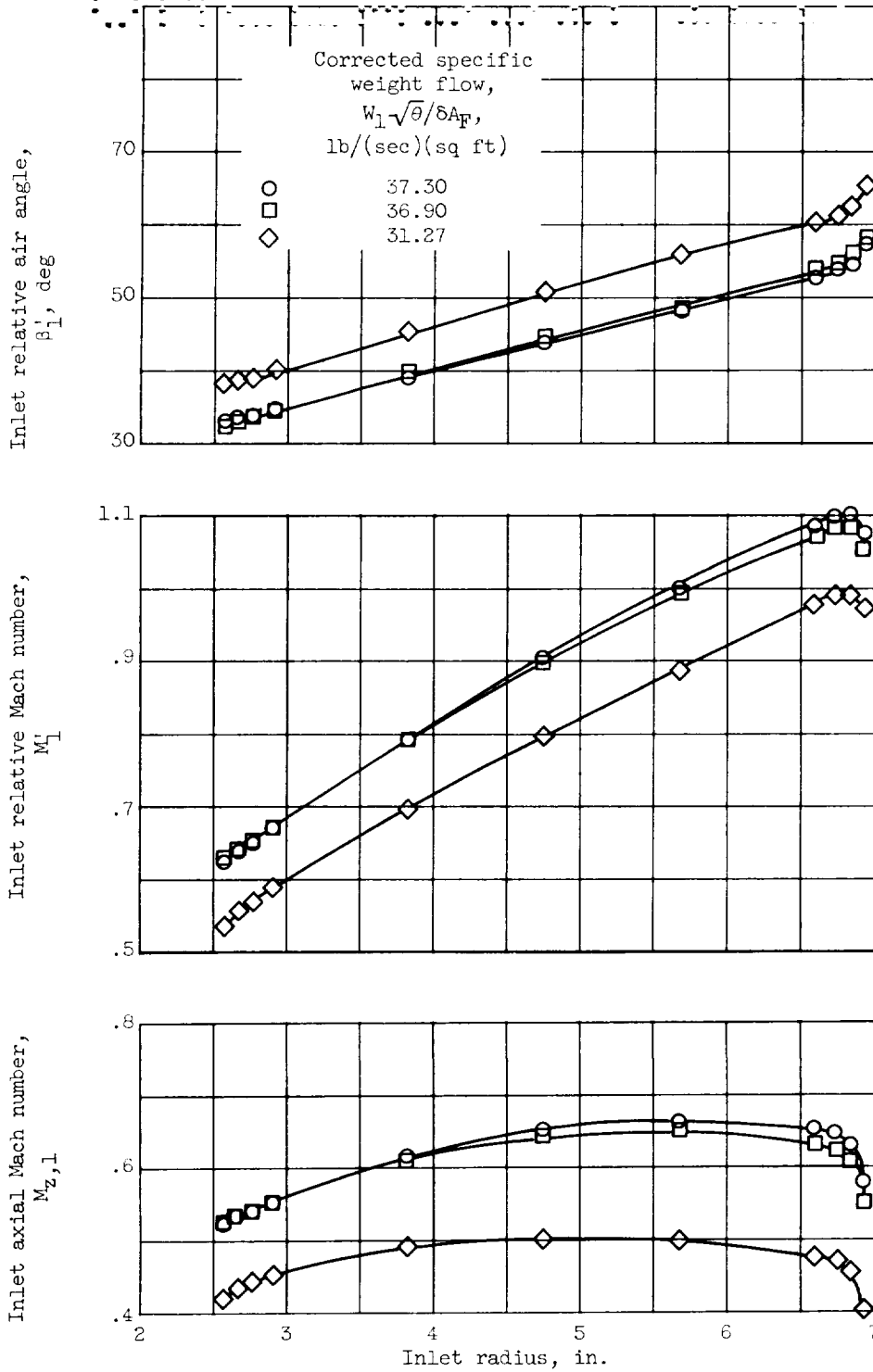
(a) Design speed.

Figure 3. - Radial variation of inlet flow parameters at various speeds.



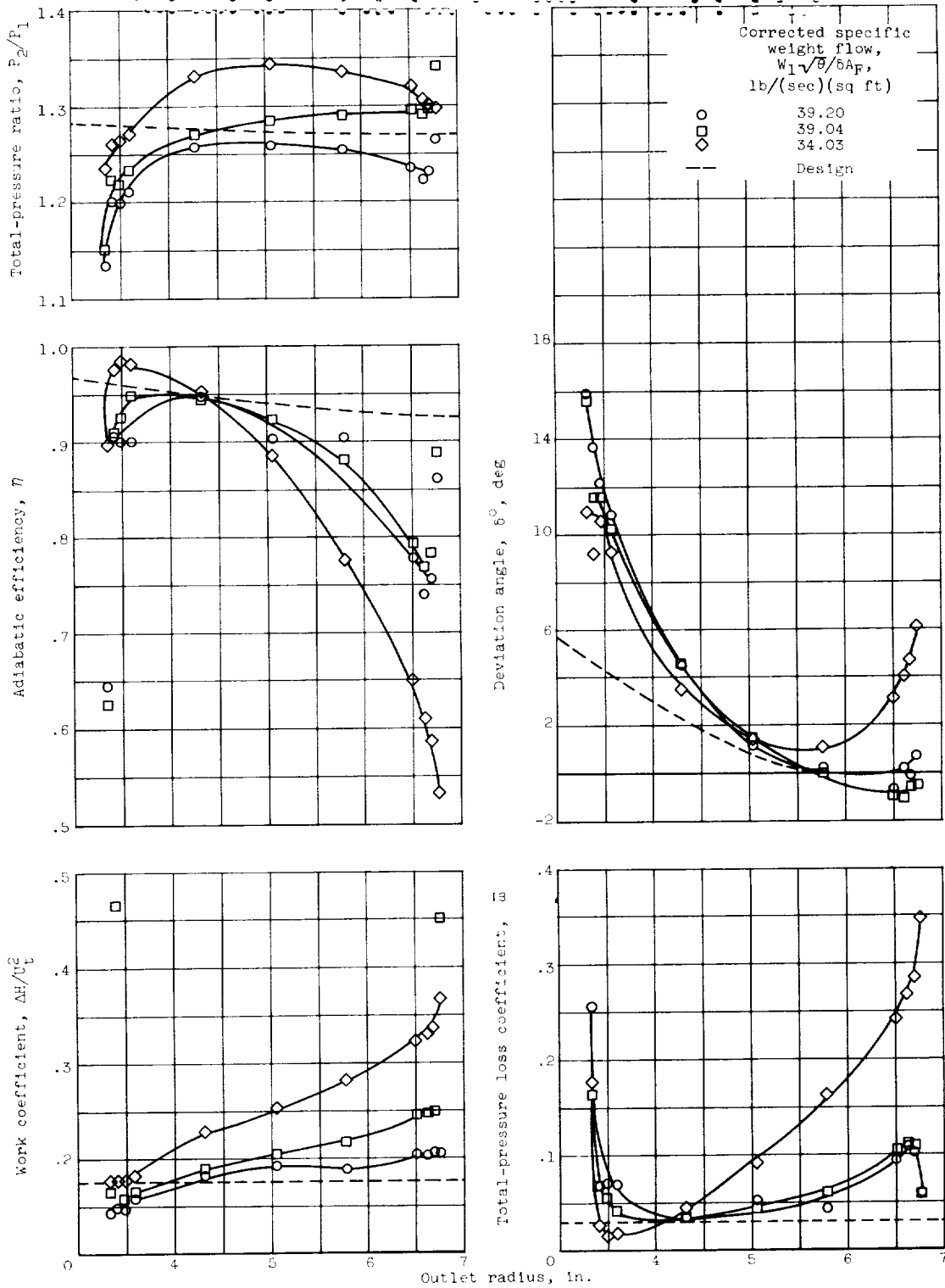
(b) 110 Percent of design speed.

Figure 3. - Continued. Radial variation of inlet flow parameters at various speeds.



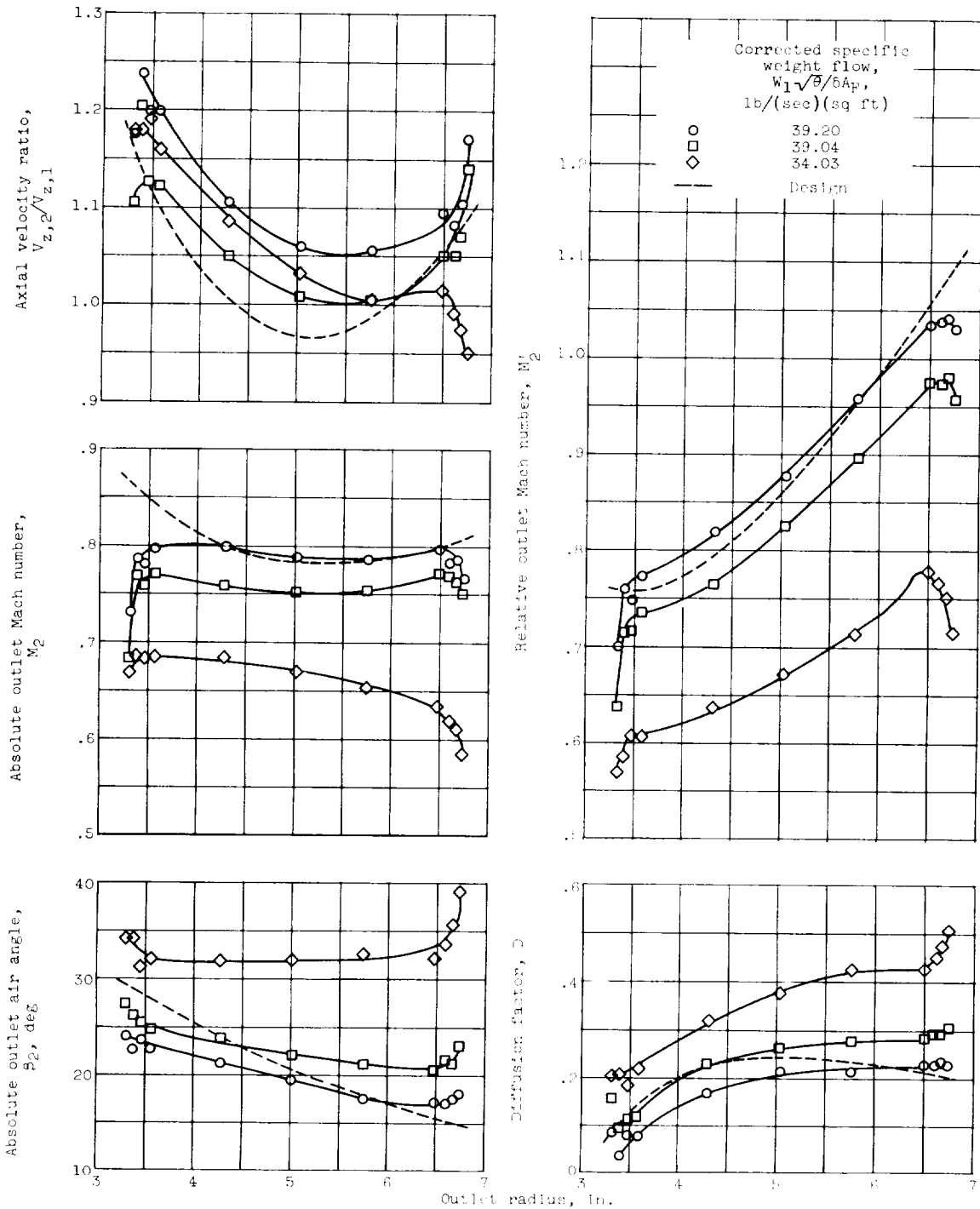
(c) 90 Percent of design speed.

Figure 3. - Concluded. Radial variation of inlet flow parameters at various speeds.



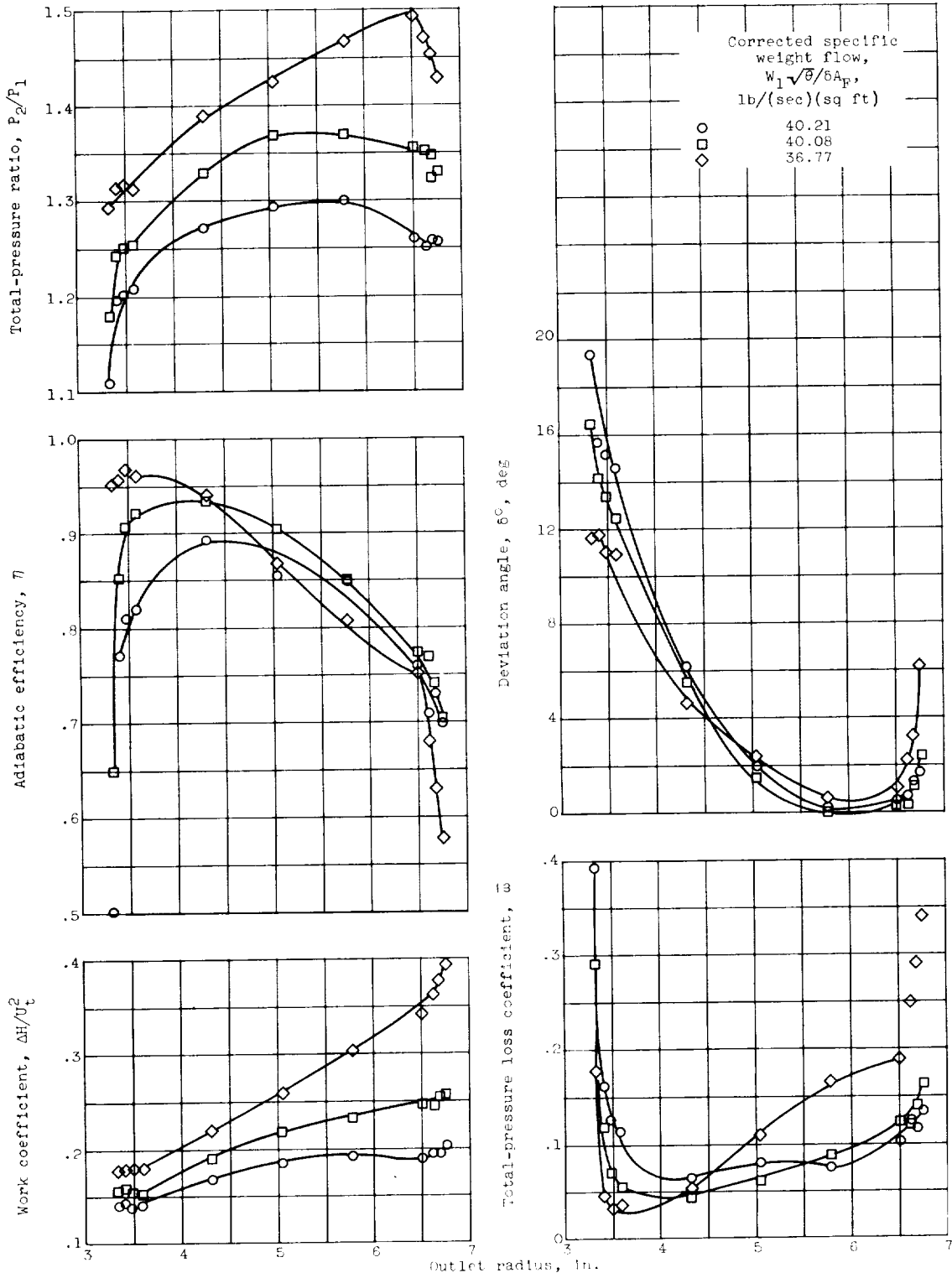
(a) Design speed.

Figure 4. - Radial variation of blade element and rotor outlet performance at various speeds.



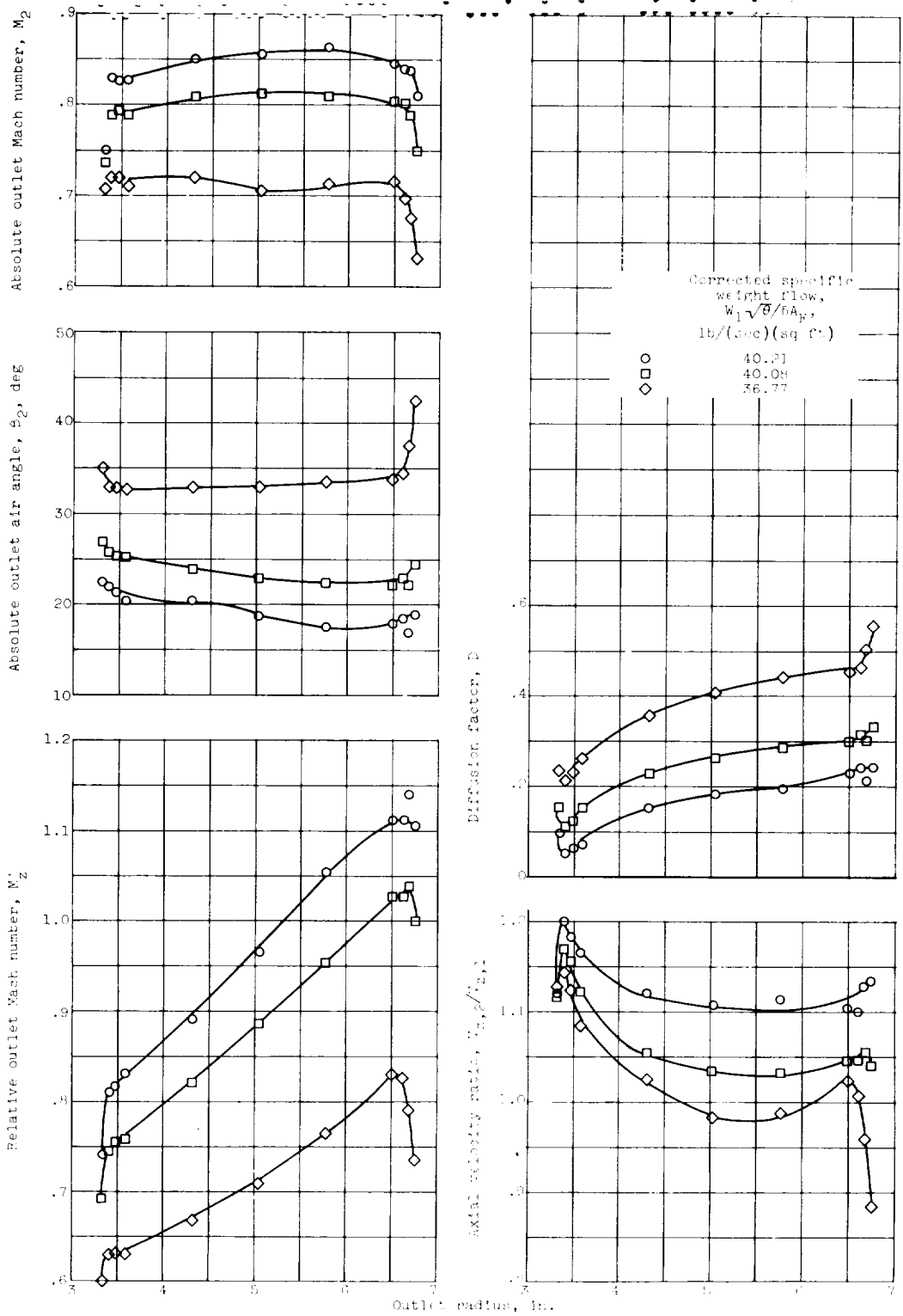
(a) Concluded. Design speed.

Figure 4. - Continued. Radial variation of blade element and rotor outlet performance at various speeds.



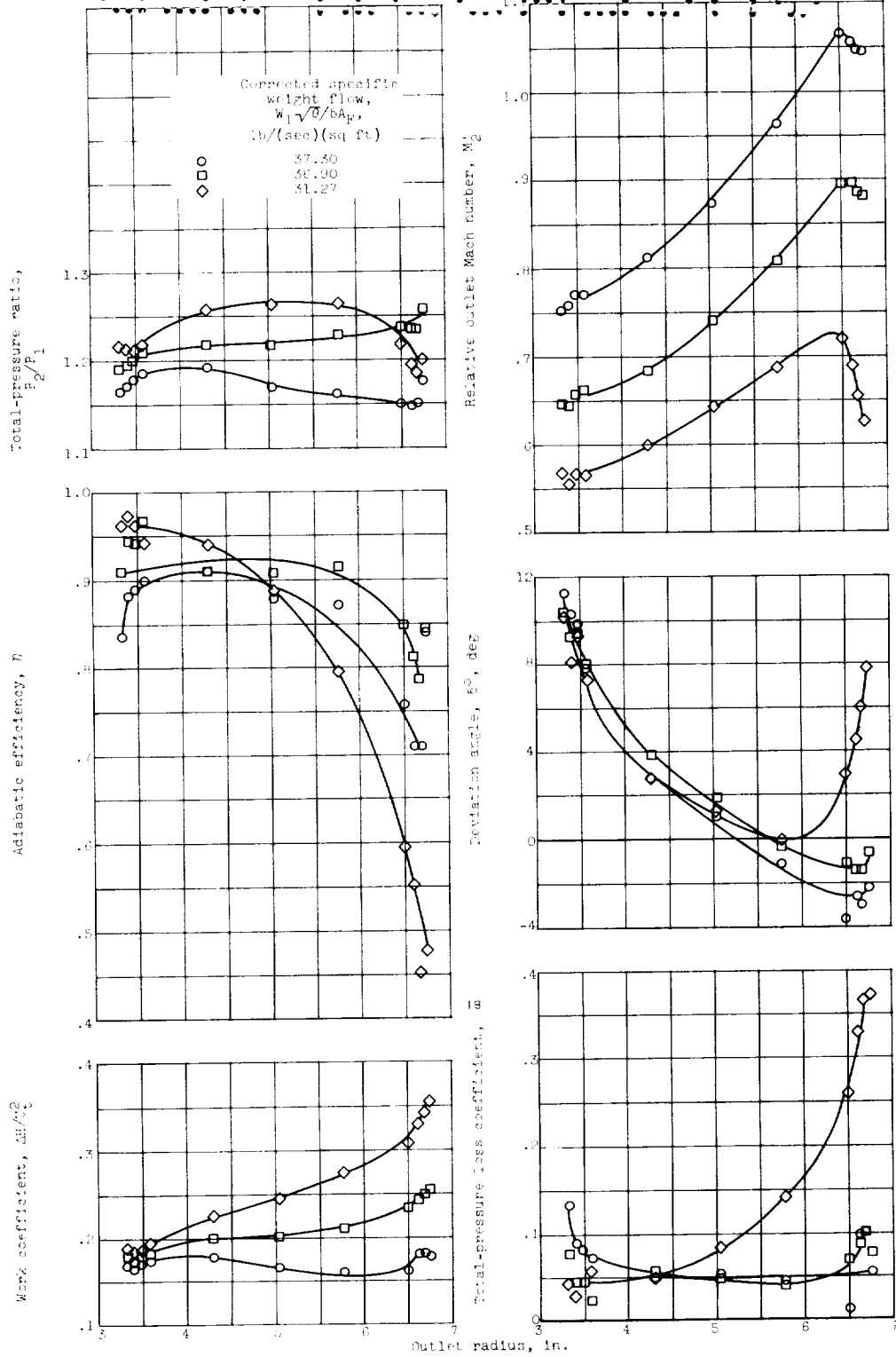
(b) 110 Percent of design speed.

Figure 4. - Continued. Radial variation of blade element and rotor-outlet performance.



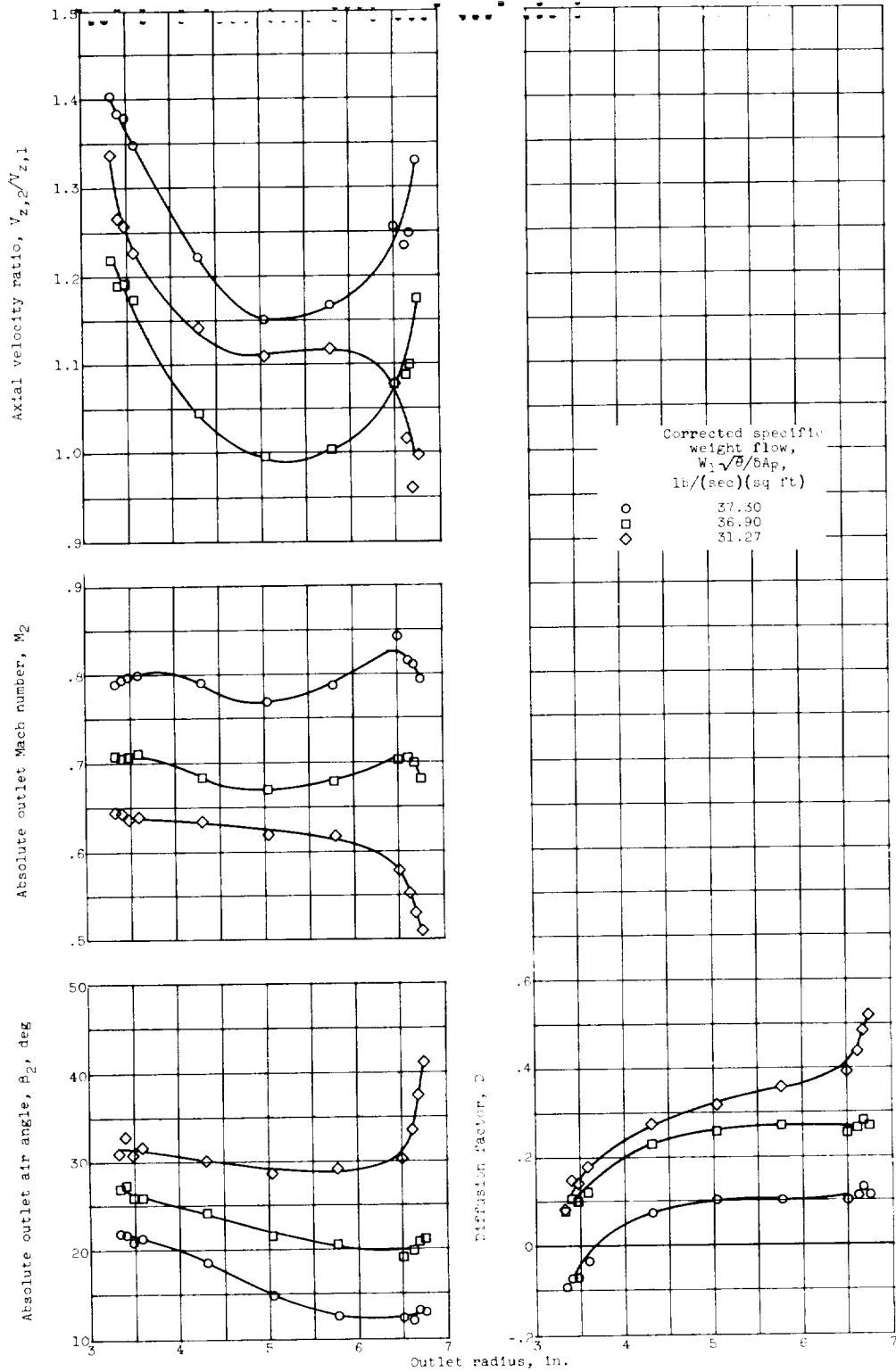
(b) Concluded. 110 Percent of design speed.

Figure 4. - Continued. Radial variation of blade element and rotor outlet performance at various speeds.



(c) 90 Percent of design speed.

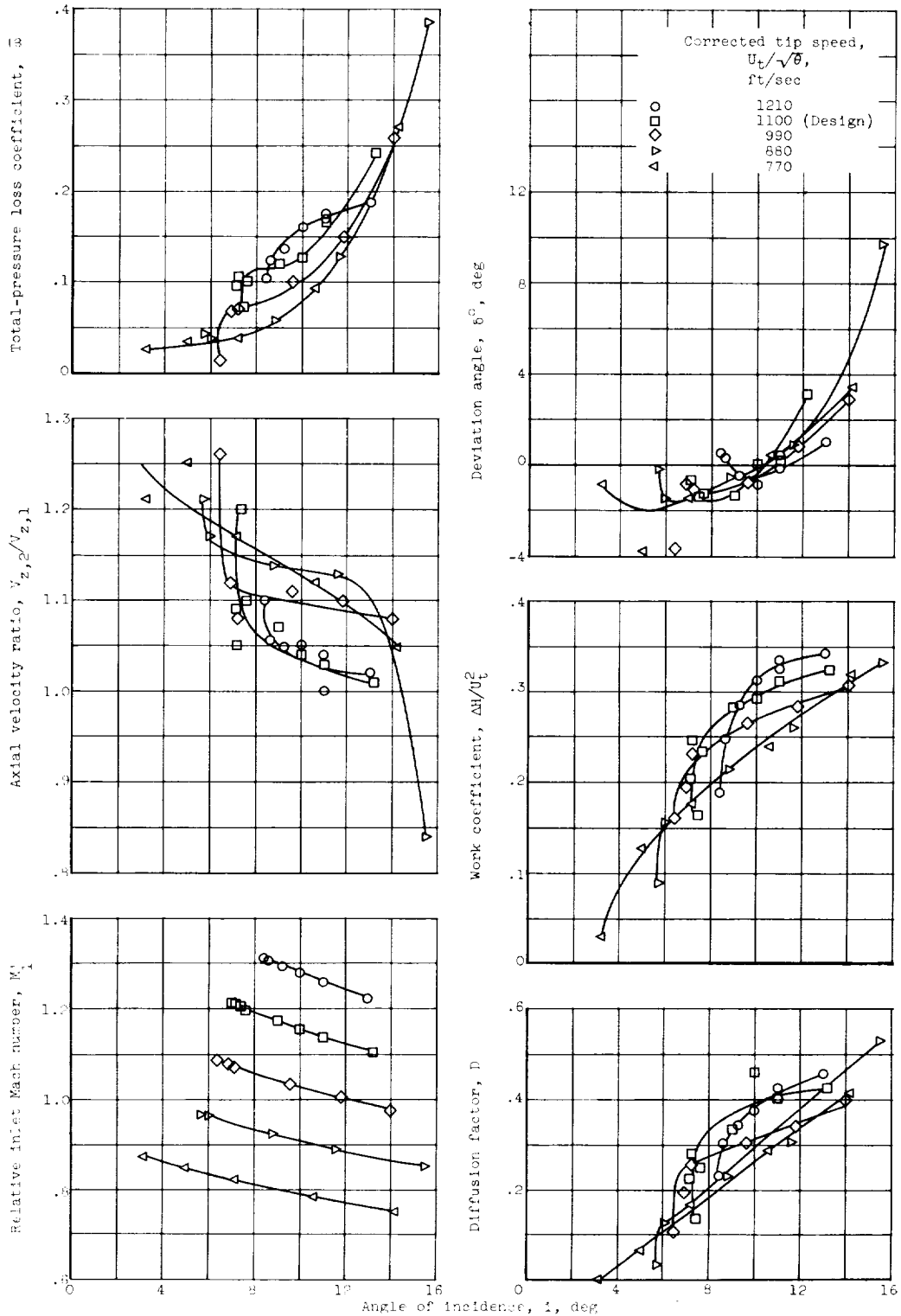
Figure 4. - Continued. Radial variation of blade element and rotor outlet performance at various speeds.



(c) Concluded. 90 Percent of design speed.

Figure 4. - Concluded. Radial variation of blade element and rotor outlet performance.

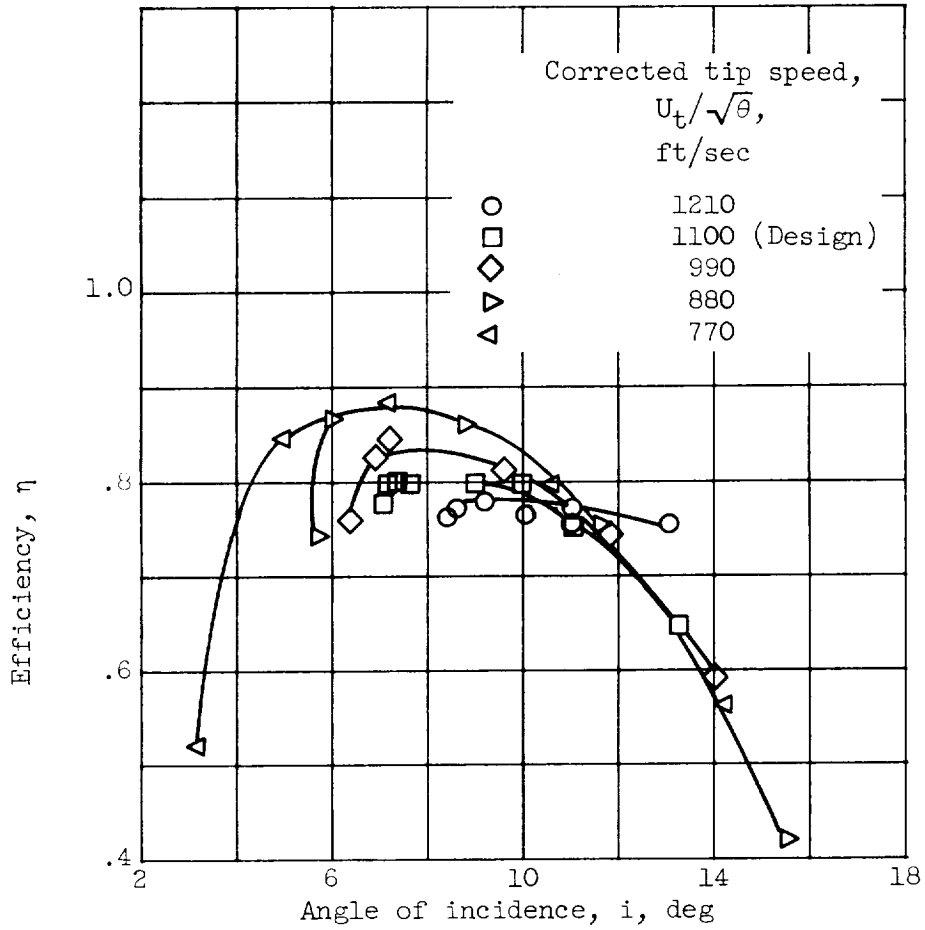
CONFIDENTIAL



(a) Radial position A; radius, 6.54 inches.

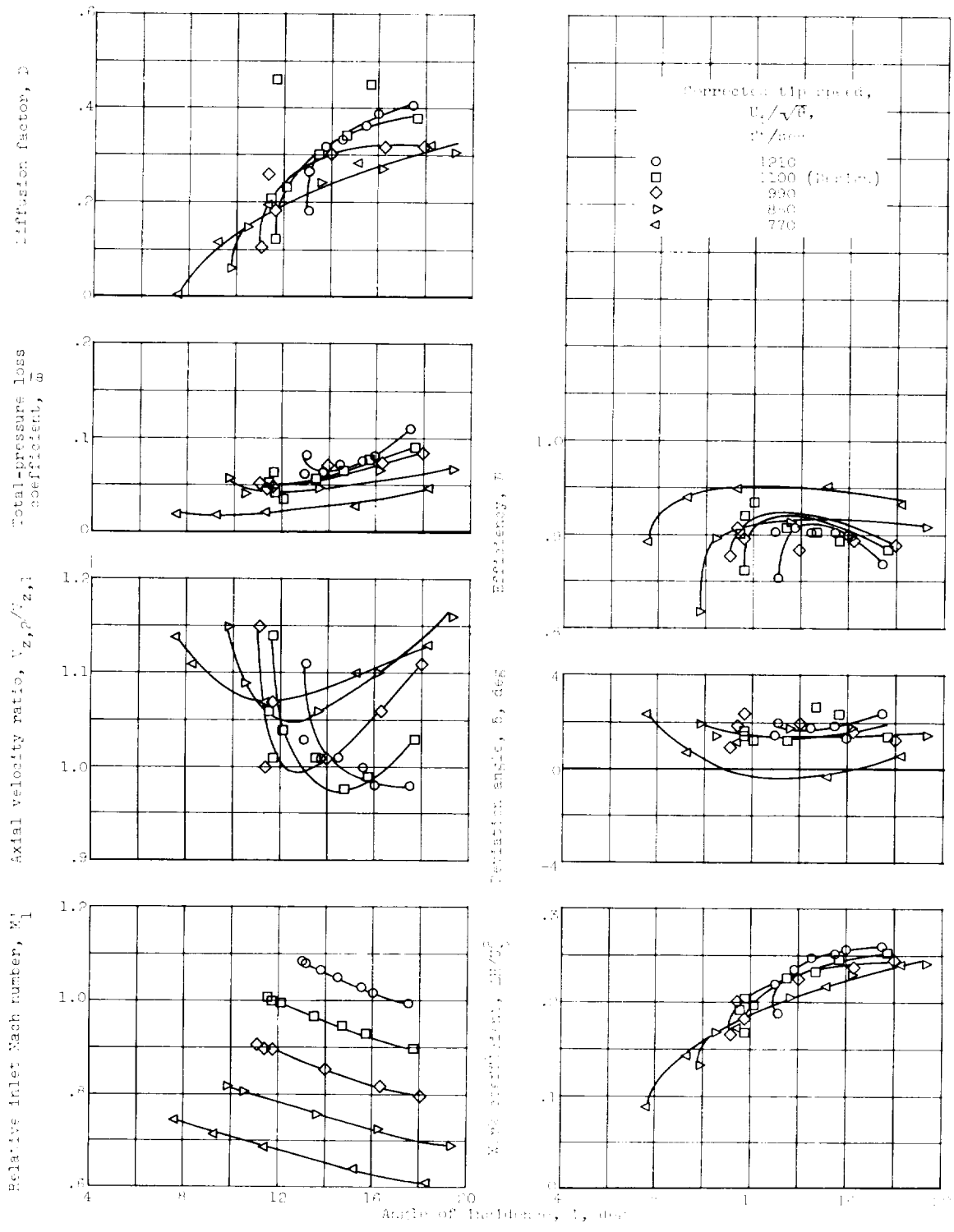
Figure 5. - Rotor blade element data.

CONFIDENTIAL



(a) Concluded. Radial position A; radius, 6.54 inches.

Figure 5. - Continued. Rotor blade element data.



(c) Saddle position by radius, 4.78 inches.

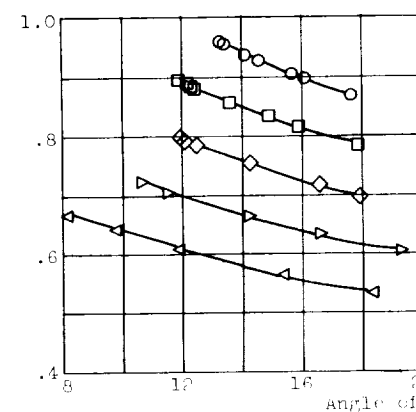
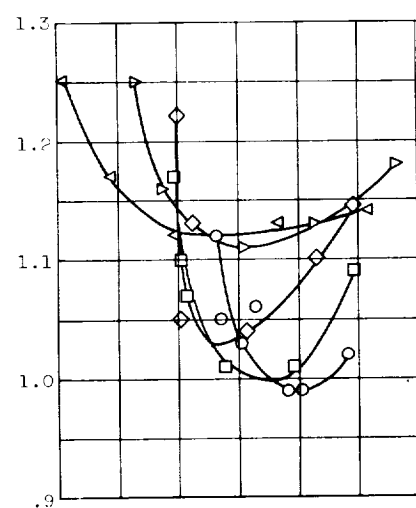
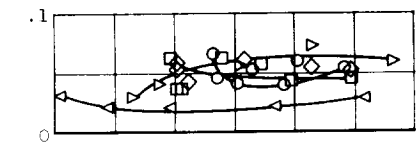
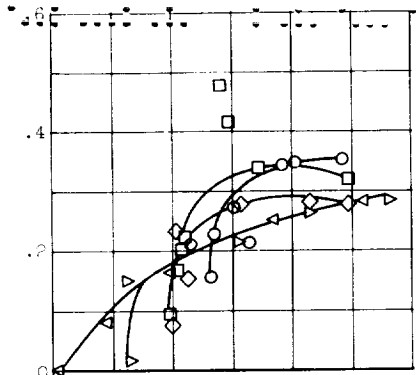
Figure 1. - Continued. (Zeta) (See caption of page 32.)

Diffusion factor, D

Total-
pressure loss-
coefficient, ω

Axial velocity ratio, $V_z, z' / V_z, 1$

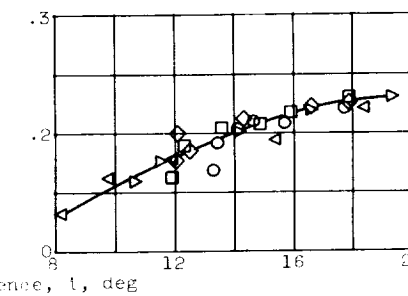
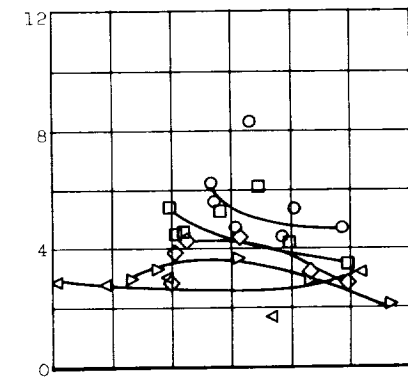
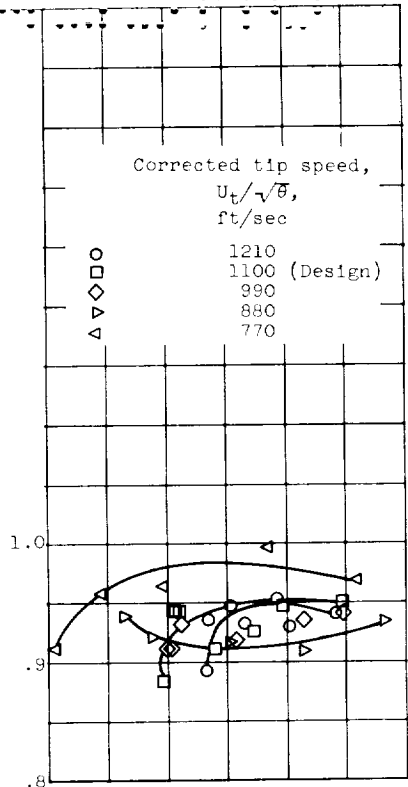
Relative inlet Mach number, M_1



Efficiency, η

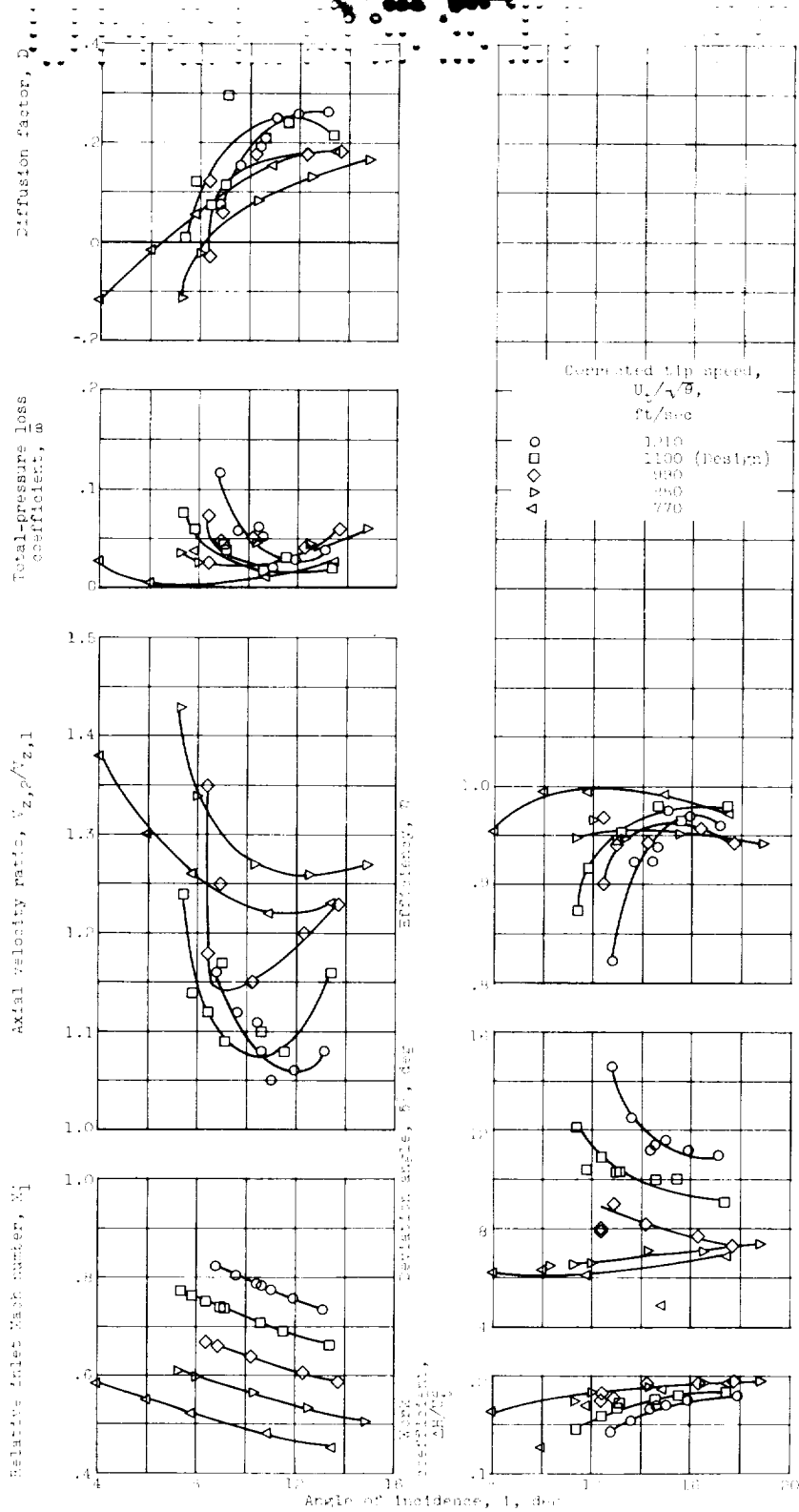
Deviation angle, δ° , deg

Work coefficient, $\Delta h / U_t^2$



(d) Radial position D; radius, 3.82 inches.

Figure 5. - Continued. Rotor blade element data.



(c) Radial position: R ; radius, 0.21 inches.

Figure 8. - Concluded. Rotor blade element data.

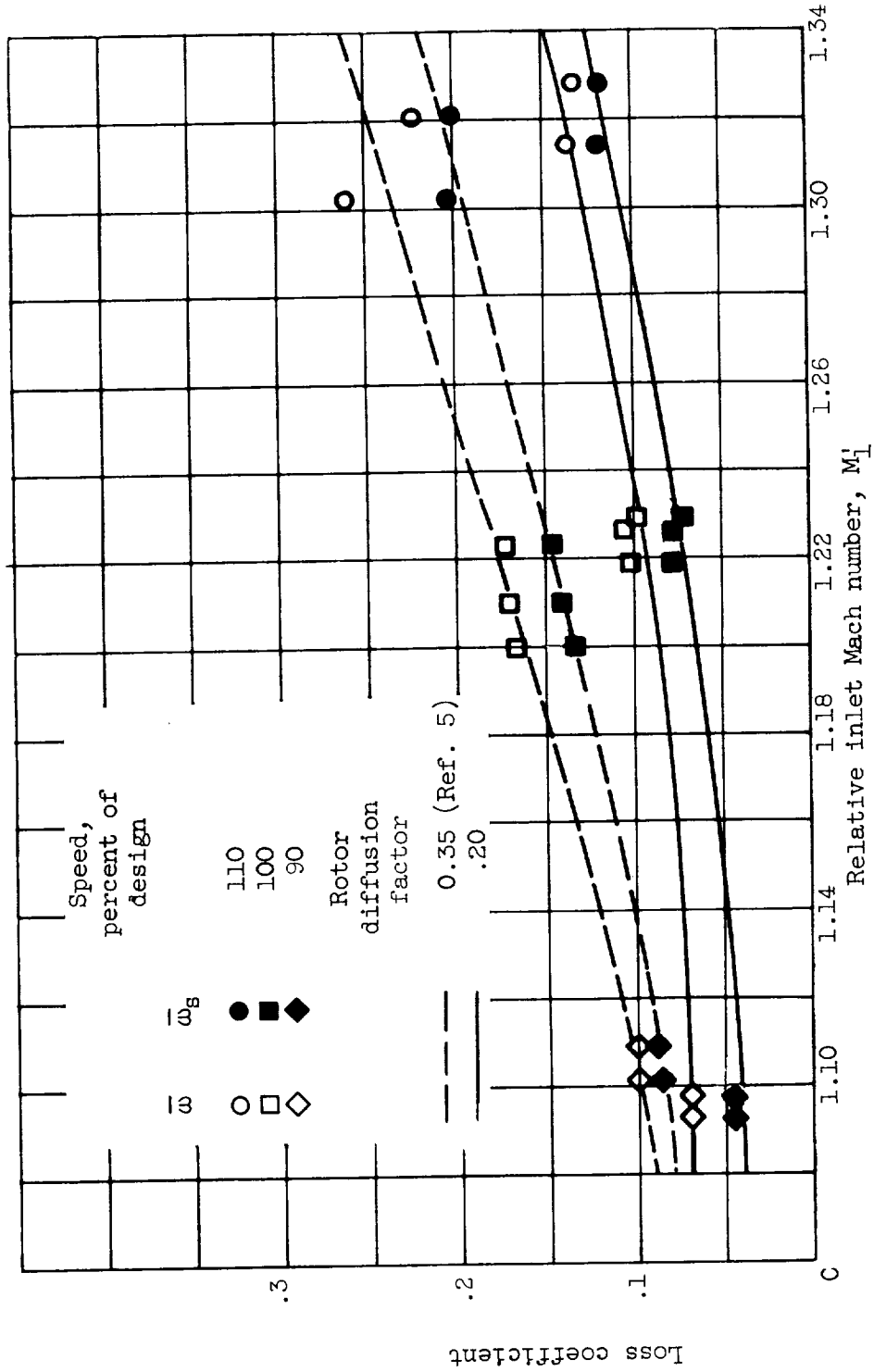


Figure 6. - Variation of total-pressure and shock loss coefficients with relative inlet Mach numbers at rotor tip section for near-peak-efficiency weight flow points at 90, 100, and 110 percent of design speed.

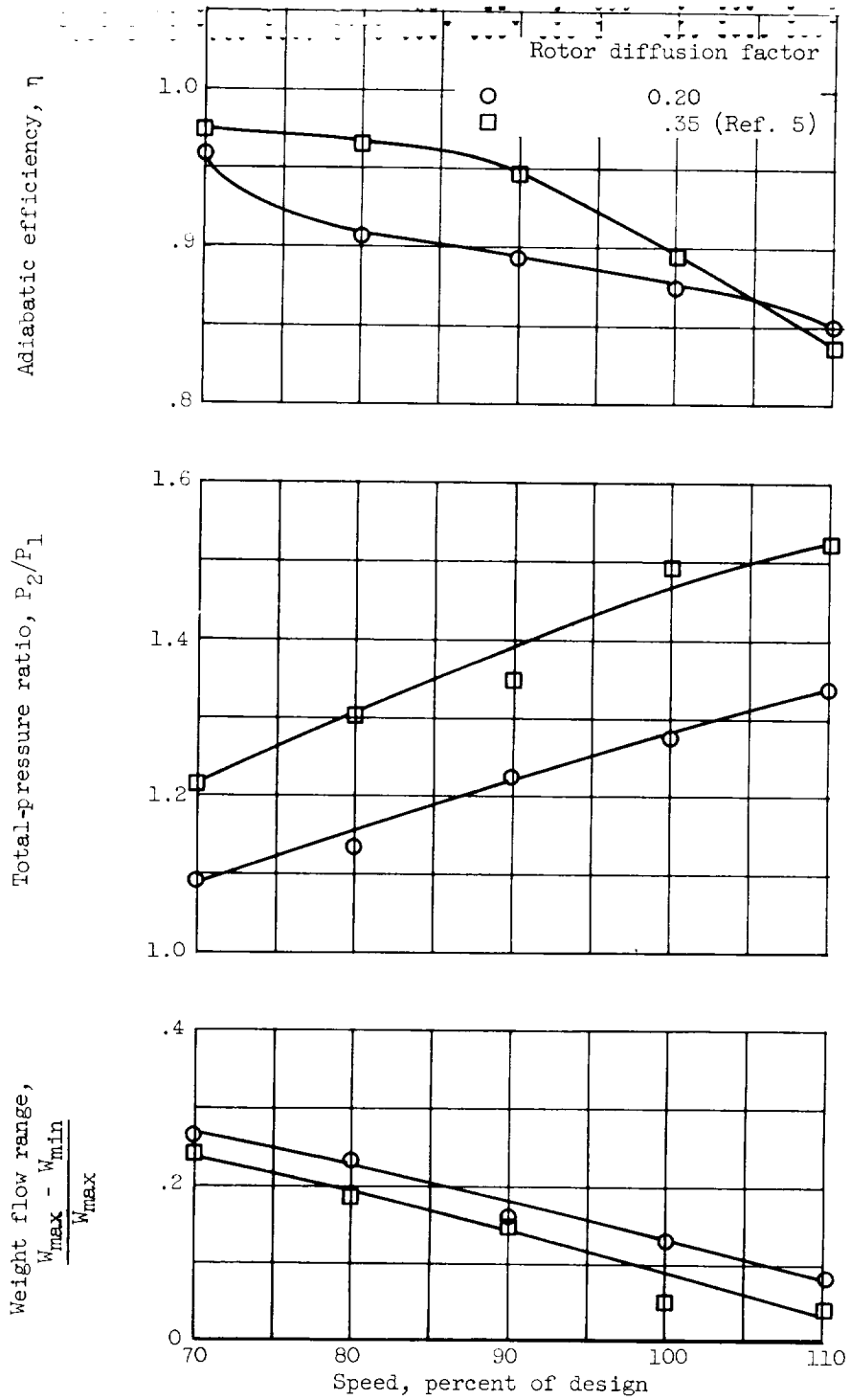


Figure 7. - Comparison of performance at peak efficiency weight flow points between rotor with 0.20 diffusion factor and rotor with 0.35 diffusion factor (ref. 5).

03171230 1040

<p>NASA TM X-86 National Aeronautics and Space Administration. EXPERIMENTAL INVESTIGATION OF A 0.35 HUB-TIP RADIUS RATIO TRANSONIC AXIAL FLOW ROTOR DESIGNED FOR 40 POUNDS PER SECOND PER SQUARE FOOT WITH A DESIGN TIP DIFFUSION FACTOR OF 0.20. Paul T. Yasaki and John C. Montgomery. September 1959. 37p. diags., tab. (NASA TECHNICAL MEMORANDUM X-86)</p> <p style="text-align: center;">CONFIDENTIAL</p> <p>(Title, Unclassified)</p> <p>In order to determine the effect of a low design diffusion factor on the performance of a transonic rotor, a high-specific-flow rotor with low blade loading was designed and tested. The design, rotor performance, and blade element performance with a discussion on rotor shock losses are presented and also a comparison with a similarly designed but more highly loaded rotor. The comparison of rotors indicates that higher blade loading offers a more desirable rotor because of a higher pressure ratio and equivalent efficiency.</p> <p style="text-align: right;">Copies obtainable from NASA, Washington</p>	<p style="text-align: center;">CONFIDENTIAL</p> <p>1. Compressors - Axial-Flow (3.6.1.1)</p> <p>I. Yasaki, Paul T. II. Montgomery, John C. III. NASA TM X-86</p>	<p>NASA TM X-86 National Aeronautics and Space Administration. EXPERIMENTAL INVESTIGATION OF A 0.35 HUB-TIP RADIUS RATIO TRANSONIC AXIAL FLOW ROTOR DESIGNED FOR 40 POUNDS PER SECOND PER SQUARE FOOT WITH A DESIGN TIP DIFFUSION FACTOR OF 0.20. Paul T. Yasaki and John C. Montgomery. September 1959. 37p. diags., tab. (NASA TECHNICAL MEMORANDUM X-86)</p> <p style="text-align: center;">CONFIDENTIAL</p> <p>(Title, Unclassified)</p> <p>In order to determine the effect of a low design diffusion factor on the performance of a transonic rotor, a high-specific-flow rotor with low blade loading was designed and tested. The design, rotor performance, and blade element performance with a discussion on rotor shock losses are presented and also a comparison with a similarly designed but more highly loaded rotor. The comparison of rotors indicates that higher blade loading offers a more desirable rotor because of a higher pressure ratio and equivalent efficiency.</p> <p style="text-align: right;">Copies obtainable from NASA, Washington</p>	<p style="text-align: center;">CONFIDENTIAL</p> <p>1. Compressors - Axial-Flow (3.6.1.1)</p> <p>I. Yasaki, Paul T. II. Montgomery, John C. III. NASA TM X-86</p>	<p style="text-align: center;">CONFIDENTIAL</p> <p>1. Compressors - Axial-Flow (3.6.1.1)</p> <p>I. Yasaki, Paul T. II. Montgomery, John C. III. NASA TM X-86</p>
<p>NASA TM X-86 National Aeronautics and Space Administration. EXPERIMENTAL INVESTIGATION OF A 0.35 HUB-TIP RADIUS RATIO TRANSONIC AXIAL FLOW ROTOR DESIGNED FOR 40 POUNDS PER SECOND PER SQUARE FOOT WITH A DESIGN TIP DIFFUSION FACTOR OF 0.20. Paul T. Yasaki and John C. Montgomery. September 1959. 37p. diags., tab. (NASA TECHNICAL MEMORANDUM X-86)</p> <p style="text-align: center;">CONFIDENTIAL</p> <p>(Title, Unclassified)</p> <p>In order to determine the effect of a low design diffusion factor on the performance of a transonic rotor, a high-specific-flow rotor with low blade loading was designed and tested. The design, rotor performance, and blade element performance with a discussion on rotor shock losses are presented and also a comparison with a similarly designed but more highly loaded rotor. The comparison of rotors indicates that higher blade loading offers a more desirable rotor because of a higher pressure ratio and equivalent efficiency.</p> <p style="text-align: right;">Copies obtainable from NASA, Washington</p>	<p style="text-align: center;">CONFIDENTIAL</p> <p>1. Compressors - Axial-Flow (3.6.1.1)</p> <p>I. Yasaki, Paul T. II. Montgomery, John C. III. NASA TM X-86</p>	<p>NASA TM X-86 National Aeronautics and Space Administration. EXPERIMENTAL INVESTIGATION OF A 0.35 HUB-TIP RADIUS RATIO TRANSONIC AXIAL FLOW ROTOR DESIGNED FOR 40 POUNDS PER SECOND PER SQUARE FOOT WITH A DESIGN TIP DIFFUSION FACTOR OF 0.20. Paul T. Yasaki and John C. Montgomery. September 1959. 37p. diags., tab. (NASA TECHNICAL MEMORANDUM X-86)</p> <p style="text-align: center;">CONFIDENTIAL</p> <p>(Title, Unclassified)</p> <p>In order to determine the effect of a low design diffusion factor on the performance of a transonic rotor, a high-specific-flow rotor with low blade loading was designed and tested. The design, rotor performance, and blade element performance with a discussion on rotor shock losses are presented and also a comparison with a similarly designed but more highly loaded rotor. The comparison of rotors indicates that higher blade loading offers a more desirable rotor because of a higher pressure ratio and equivalent efficiency.</p> <p style="text-align: right;">Copies obtainable from NASA, Washington</p>	<p style="text-align: center;">CONFIDENTIAL</p> <p>1. Compressors - Axial-Flow (3.6.1.1)</p> <p>I. Yasaki, Paul T. II. Montgomery, John C. III. NASA TM X-86</p>	<p style="text-align: center;">CONFIDENTIAL</p> <p>1. Compressors - Axial-Flow (3.6.1.1)</p> <p>I. Yasaki, Paul T. II. Montgomery, John C. III. NASA TM X-86</p>

031712501040